

The $\langle A^2 \rangle$ asymmetry and propagators in lattice $SU(2)$ gluodynamics at $T > T_c$.

V. G. Bornyakov

Institute for High Energy Physics NRC Kurchatov Institute, 142281 Protvino, Russia

School of Biomedicine, Far East Federal University, 690950 Vladivostok, Russia

Institute of Theoretical and Experimental Physics NRC Kurchatov Institute, 117259 Moscow, Russia

V. K. Mitrjushkin

Joint Institute for Nuclear Research, 141980 Dubna, Russia

and Institute of Theoretical and Experimental Physics NRC Kurchatov Institute, 117259 Moscow, Russia

R. N. Rogalyov

Institute for High Energy Physics NRC Kurchatov Institute,

142281 Protvino, Russia

We study numerically the chromoelectric-chromomagnetic asymmetry of the dimension two A^2 gluon condensate as well as the *transverse and longitudinal* gluon propagators at $T > T_c$ in the Landau-gauge $SU(2)$ lattice gauge theory with a particular emphasis on finite-volume effects. We show that previously found so called symmetric point at which asymmetry changes sign is an artifact of the finite volume effects. We find that with increasing temperature the asymmetry decreases approaching zero value from above in agreement with perturbative result. Instead of the asymmetry we suggest the ratio of the transverse to longitudinal propagator taken at zero momentum as an indicator of the boundary of the postconfinement domain and find it at $T \simeq 1.7T_c$.

PACS numbers: 11.15.Ha, 12.38.Gc, 12.38.Aw

Keywords: Lattice gauge theory, finite temperature, gluon propagator, dimension 2 gluon condensate

I. INTRODUCTION

Studies of the dimension-two gauge-boson condensate

$$\langle A^2 \rangle = g^2 \langle A_\mu^a(x) A_\mu^a(x) \rangle \quad (1)$$

in the last 15 years were initiated by the Ref. [1], where it was shown that the nonperturbative part of $\langle A^2 \rangle$ is completely determined by contribution of the topological defects (monopoles) responsible for confinement in the compact electrodynamics. Since monopole condensation is one of the most popular scenarios of confinement also in nonabelian gauge theories, this observation suggested that the gluon dimension-two condensate plays an important role in the studies of infrared properties of Yang–Mills theories as well.

In spite of some earlier considerations of the composite operator $A^2(x) = A_\mu^a(x) A_\mu^a(x)$ ([2] *etc*), for long time it was disregarded in the OPE approach because of its gauge dependence.

In the Landau gauge, the operator $A^2(x)$ is BRST invariant (on mass shell) and multiplicatively renormalizable, as was shown in [3, 4] in the \overline{MS} scheme. Later it was argued [5] that the matrix element $\langle A^2 \rangle$ is gauge-invariant in spite of gauge dependence of the respective operator, still it does not appear in the expansions of products of gauge-invariant composite operators [6].

The effective potential for $\langle A^2 \rangle$ was obtained in [3, 7] indicating nonvanishing value of $\langle A^2 \rangle$ and thus

dynamical gluon mass generation.

In the OPE approach, $\langle A^2 \rangle$ was used for the parametrization of soft nonperturbative contributions to the Green functions, for a review see [8]. Thus it was extracted from their high momentum behavior [9, 10].

It was shown that, over the momentum range $2.5 \div 7$ GeV, ghost and gluon propagators evaluated on a lattice agree with the respective perturbative estimates only when corrections due to $\langle A^2 \rangle$ condensate are taken into account [11, 12].

In a series of papers (see e.g. [8, 13] and references therein) $\langle A^2 \rangle$ was computed numerically from fits to lattice data for the gluon and ghost propagators as well as 3-gluon and ghost-gluon vertices. For example, in a specific MOM-type renormalization scheme defined by a zero incoming ghost momentum¹ ($\mu = 10$ GeV), the following values for the $N_f = 2 + 1 + 1$ QCD were found [14]:

$$\langle A^2 \rangle = 2.8(8) \text{ GeV}^2 \quad (\text{OPE up to } \frac{1}{p^4})$$

$$\langle A^2 \rangle = 3.8(6) \text{ GeV}^2 \quad (\text{OPE up to } \frac{1}{p^6})$$

in order to obtain the QCD coupling constant $\alpha_{\overline{MS}}(M_Z) = 0.1198(4)(8)(6)$.

The $\langle A^2 \rangle$ condensate was also intensively studied

¹ Also referred to as the Taylor scheme

in the refined Gribov-Zwanziger (RGZ) approach [15–17]. Other studies of this condensate include [18–20].

In Ref. [1] the $\langle A^2 \rangle$ was related to the confinement-deconfinement transition in 4D compact $U(1)$ gauge theory. In this theory the confinement and deconfinement phases are separated by the phase transition at zero temperature. It was found that the nonperturbative part of the condensate drops at critical coupling. This observation raised hopes that the $\langle A^2 \rangle$ condensate might be also of relevance for the finite temperature transition in the 4D non-Abelian theories.

There are two A^2 condensates at nonzero temperature, electric $\langle A_E^2 \rangle$ and magnetic $\langle A_M^2 \rangle$:

$$\begin{aligned}\langle A_E^2 \rangle &= g^2 \langle A_4^a(x) A_4^a(x) \rangle, \\ \langle A_M^2 \rangle &= g^2 \langle A_i^a(x) A_i^a(x) \rangle.\end{aligned}\quad (2)$$

The quantity of particular interest is the (color) electric-magnetic asymmetry introduced in [21]:

$$\langle \Delta_{A^2} \rangle \equiv \langle A_E^2 \rangle - \frac{1}{3} \langle A_M^2 \rangle. \quad (3)$$

Later we will also use the dimensionless quantity

$$\mathcal{A} = \frac{\langle \Delta_{A^2}(x) \rangle}{T^2}. \quad (4)$$

Within the OPE approach and in the $p_4 = 0$ approximation, it was shown [22] that the asymmetry contributes to the quark propagator at nonzero temperatures.

The main interest in the asymmetry stems from its possible relation to both the confinement-deconfinement transition and dynamics in the deconfinement phase.

There is some range of temperature values just above T_c , where the quark-gluon plasma (QGP) demonstrates special properties and cannot be treated perturbatively see e.g. [23]. In particular the QGP pressure differs from the ideal-gas value. In the $SU(3)$ theory, an indication of this range is also provided by the behavior of the renormalized Polyakov loop, which jumps from zero to only ~ 0.4 at $T = T_c$ and then increases with temperature over the range $T_c < T < 4T_c$ [24, 25]. As for the potential between heavy quarks, it was found [26] that charmonium states persist up to $T = 1.6T_c$. The range of temperatures above T_c up to $(2 \div 4)T_c$ is referred to as the postconfinement domain, and strongly interacting matter at these temperatures — as semi-QGP [27, 28]. It is often considered that color charges are unscreened in ‘total’ QGP, and partially screened in semi-QGP [29].

The postconfinement domain was also characterized in terms of density of Abelian magnetic monopoles [30, 31]. According to Ref. [31] the monopoles are condensed in the confinement phase, represent dilute gas above $2T_c$ and liquid at $T_c < T < 2T_c$. In Ref. [30] the relevance of color-magnetic and color-electric fluctuations was discussed in terms of respective couplings.

The authors also discussed the screening masses as indicators of the (in their terminology) E-M equilibrium point and argued that the temperature determined by the equality of the electric and magnetic screening masses should coincide with temperature determined by respective couplings. Using lattice results for the electric and magnetic screening masses obtained in $SU(3)$ gluodynamics [32] they concluded that this temperature is between $1.2T_c$ and $1.5T_c$.

It has long been known [33] that, over the range $T_c < T < 3T_c$, the contributions of the electric and magnetic parts of the gluon condensate

$$\langle G_{\mu\nu}^2 \rangle = \langle G_E^2 \rangle + \langle G_M^2 \rangle$$

to the energy density and pressure change with temperature much more rapidly than their sum. This gives some evidence that an interplay of electric and magnetic degrees of freedom plays an important role in the dynamics of semi-QGP.

Yet another evidence for this comes from the effective high-temperature 3D theories [34–36], in which the electric and magnetic degrees of freedom are in fact separated.

For a long time these models failed to reproduce the pressure of semi-QGP and to predict the transition to the confinement phase [37, 38]. This problem was solved with the appearance of the effective models based on the Polyakov loop [39–41], where large fluctuations of A_0 are taken into consideration. That is, dynamics just above T_c in the 3D effective models is substantially determined by the electric degrees of freedom. This resembles the above-mentioned situation with the electric and magnetic condensates in the postconfinement domain, where the magnetic contribution to the energy density and pressure only partially compensates the electric one.

In this work we employ both the asymmetry and the ratio between the transverse and longitudinal propagators in attempt to set the upper limit on the temperature range where the electric fluctuations dominate.

In [21] the asymmetry was computed for the first time in lattice $SU(2)$ gluodynamics for a wide range of temperatures in both confinement and deconfinement phases. It was found that it peaks at the phase transition and monotonically decreases with increasing temperature in the deconfinement phase. Furthermore, it was found that the asymmetry crosses zero at $T \approx 2.2T_c$ and becomes negative at higher temperatures. The existence of this symmetric point was one of the main results of Ref. [21].

In this paper we make a number of improvements in computation of the asymmetry in comparison with Ref. [21]. We take care of the finite-volume and Gribov-copy effects. As a result we demonstrate that the asymmetry is indeed monotonically decreasing function in the deconfinement phase but it never turns zero. This result is in a qualitative agreement with the perturbative calculations, see below.

Thus we demonstrate that the asymmetry cannot serve as an indicator of the boundary of the postconfinement domain. We suggest a new gluonic quantity to indicate such boundary - the ratio of the magnetic to electric propagator at zero momentum which can be related to the ratio of the respective screening masses.

II. DEFINITIONS AND SIMULATION DETAILS

We study $SU(2)$ lattice gauge theory with the standard Wilson action

$$S = \beta \sum_x \sum_{\mu > \nu} \left[1 - \frac{1}{2} \text{Tr} \left(U_{x\mu} U_{x+\mu;\nu} U_{x+\nu;\mu}^\dagger U_{x\nu}^\dagger \right) \right],$$

where $\beta = 4/g^2$ and g is a bare coupling constant. The link variables $U_{x\mu} \in SU(2)$ transform under gauge transformations ω_x as follows:

$$U_{x\mu} \xrightarrow{\omega} U_{x\mu}^\omega = \omega_x^\dagger U_{x\mu} \omega_{x+\mu}; \quad \omega_x \in SU(2). \quad (5)$$

Our calculations were performed on the asymmetric lattices with lattice volume $V = N_t \times N_s^3$, where N_t is the number of sites in the 4th direction. The temperature T is given by

$$T = \frac{1}{aN_t}, \quad (6)$$

where a is the lattice spacing. We employ the standard definition of the lattice gauge vector potential² $A_{x,\mu}$ [42]:

$$A_{x,\mu} = \frac{Z}{2ia g} \left(U_{x\mu} - U_{x\mu}^\dagger \right) \equiv A_{x,\mu}^a \frac{\sigma_a}{2}, \quad (7)$$

where Z is the renormalization factor, defined in the text after equation (15).

The lattice Landau gauge fixing condition is

$$(\nabla^B A)_x \equiv \frac{1}{a} \sum_{\mu=1}^4 (A_{x,\mu} - A_{x-a\hat{\mu},\mu}) = 0, \quad (8)$$

which is equivalent to finding an extremum of the gauge functional

$$F_U(\omega) = \frac{1}{4V} \sum_{x\mu} \frac{1}{2} \text{Tr} U_{x\mu}^\omega, \quad (9)$$

with respect to gauge transformations ω_x . After replacing $U \Rightarrow U^\omega$ at the extremum the gauge condition (8) is satisfied.

The gluon propagator $D_{\mu\nu}^{ab}(p)$ is defined as follows:

$$D_{\mu\nu}^{ab}(p) = \frac{1}{V a^4} \langle \tilde{A}_\mu^a(q) \tilde{A}_\nu^b(-q) \rangle$$

where

$$\tilde{A}_\mu^b(q) = a^4 \sum_x A_{x,\mu}^b \exp \left(i q(x + \frac{\hat{\mu} a}{2}) \right), \quad (10)$$

$q_i \in (-N_s/2, N_s/2]$ and $q_4 \in (-N_t/2, N_t/2]$. The physical momenta p_μ are defined by relations $ap_i = 2 \sin(\pi q_i/N_s)$, $ap_4 = 2 \sin(\pi q_4/N_t)$.

On the asymmetric lattice there are two tensor structures for the gluon propagator [43]:

$$D_{\mu\nu}^{ab}(p) = \delta_{ab} (P_{\mu\nu}^T(p) D_T(p) + P_{\mu\nu}^L(p) D_L(p)), \quad (11)$$

where (symmetric) orthogonal projectors $P_{\mu\nu}^{T;L}(p)$ are defined for $p = (\vec{p} \neq 0; p_4 = 0)$ as follows

$$P_{ij}^T(p) = \left(\delta_{ij} - \frac{p_i p_j}{\vec{p}^2} \right), \quad P_{\mu 4}^T(p) = 0; \quad (12)$$

$$P_{44}^L(p) = 1; \quad P_{\mu i}^L(p) = 0. \quad (13)$$

Therefore, two scalar propagators - longitudinal $D_L(p)$ and transverse $D_T(p)$ - are given by

$$\begin{aligned} D_T(p) &= \frac{1}{6} \sum_{a=1}^3 \sum_{i=1}^3 D_{ii}^{aa}(p); \\ D_L(p) &= \frac{1}{3} \sum_{a=1}^3 D_{44}^{aa}(p), \end{aligned} \quad (14)$$

For $\vec{p} = 0$ they are defined as follows:

$$\begin{aligned} D_T(0) &= \frac{1}{9} \sum_{a=1}^3 \sum_{i=1}^3 D_{ii}^{aa}(0), \\ D_L(0) &= \frac{1}{3} \sum_{a=1}^3 D_{00}^{aa}(0). \end{aligned} \quad (15)$$

$D_T(p)$ is associated with the magnetic sector, $D_L(p)$ - with the electric sector.

We consider both bare quantities (either labeled by index *bare* or without index) and renormalized quantities (labelled by index *MOM*). The renormalization factor (see equation (7)) for bare quantities is equal to unity $Z \equiv Z_{bare} = 1$. For renormalized quantities $Z \equiv Z_{MOM}$ and is defined by the requirement

$$D_L^{MOM}(p^2 = \mu^2) = \frac{1}{\mu^2}, \quad (16)$$

² In perturbation theory, $A_{x+\hat{\mu}/2,\mu}$ instead of $A_{x,\mu}$ provides a more adequate designation; $\hat{\mu}$ is the unit vector in the μ th direction.

with normalization point $\mu = 3$ GeV.

In terms of lattice variables, the asymmetry has the form

$$\mathcal{A} = \frac{4a^2 N_t^2}{\beta} \sum_{b=1}^3 \left(\left\langle A_{x,4}^b A_{x,4}^b \right\rangle - \frac{1}{3} \sum_{i=1}^3 \left\langle A_{x,i}^b A_{x,i}^b \right\rangle \right), \quad (17)$$

It can be expressed in terms of the gluon propagators:

$$\mathcal{A} = \frac{4N_t}{\beta a^2 N_s^3} \left[3(D_L(0) - D_T(0)) + \sum_{p \neq 0} \left(\frac{3|\vec{p}|^2 - p_4^2}{p^2} D_L(p) - 2D_T(p) \right) \right] \quad (18)$$

In the continuum limit, the respective integral is ultra-violate finite [21, 44]; therefore, no additional renormalization is needed and this formula holds true for renormalized quantities as well. Thus the asymmetry \mathcal{A} , which is nothing but the vacuum expectation value of the respective composite operator, is multiplicatively renormalizable and its renormalization factor coincides with that of the propagator³.

The authors of [44] obtained one-loop perturbative estimates of the asymmetry both at high temperatures

$$\langle \Delta_{A^2} \rangle \simeq \frac{g^2 T^2}{4} \left(1 - \frac{g}{3\pi} \sqrt{\frac{2}{3}} \right) \quad (19)$$

and at low temperatures

$$\langle \Delta_{A^2} \rangle \simeq \frac{g^2 \pi^2}{10} \left(1 - \frac{85}{522} \frac{g^2}{16\pi^2} \right) \frac{T^4}{M^2}, \quad (20)$$

where

$$M^2 = -\frac{13}{54} \langle A^2(T=0) \rangle.$$

We have generated ensembles of $O(1500)$ independent Monte Carlo lattice field configurations. Consecutive configurations (considered as independent) were separated by $100 \div 200$ (for $N_s = 24 \div 84$) sweeps, each sweep consisting of one local heatbath update followed by $N_s/2$ microcanonical updates. In Table VII we provide information about the ensembles used throughout this paper.

In the gauge fixing procedure we employ the $Z(2)$ transformation proposed in [45]. $Z(2)$ flip in direction μ consists in flipping all link variables $U_{x\mu}$ attached and orthogonal to a 3d plane by multiplying them with -1 . Such global flips are equivalent to non-periodic gauge transformations and represent an exact symmetry of the pure gauge action. The Polyakov loops in

the direction of the chosen links and averaged over the 3d plane obviously change their sign. At finite temperature we apply flips only to directions $\mu = 1, 2, 3$, thus we consider 8 flip sectors. In the deconfinement phase, where the $Z(2)$ symmetry is broken, the $Z(2)$ sector of the Polyakov loop in the $\mu = 4$ direction has to be chosen since on large enough volumes all lattice configurations belong to the same sector, i.e. there are no flips between sectors in the Markov chain of configurations. We choose the sector with positive Polyakov loop.

Following Ref. [46] in what follows we call the combined gauge fixing algorithm employing simulated annealing (SA) algorithm (with finalizing overrelaxation) and $Z(2)$ flips for space directions the ‘FSA’ algorithm. We generated $n_{copy} = 1$ to 3 gauge copies per flip-sector each time starting from a random gauge transformation of the Monte Carlo configuration, obtaining in this way $N_{copy} = 8n_{copy}$ Landau-gauge fixed copies for every configuration. We take the copy with maximal value of the functional (9) as our best estimator of the global maximum and denote it as best (“bc”) copy. In order to demonstrate the Gribov copy effect we compare with the results obtained from the randomly chosen first (“fc”) copy and with the ‘worst’ copy (“wc”), i.e. copy with the lowest value of the gauge functional.

To suppress ‘geometrical’ lattice artifacts, we apply the “ α -cut” [47], i.e. $\pi q_i / N_s < \alpha$, for every component, in order to keep close to a linear behavior of the lattice momenta $p_i \approx (2\pi q_i) / (aN_s)$, $q_i \in (-N_s/2, N_s/2]$. We have chosen $\alpha = 0.5$. Obviously, this cut influences large momenta only. We did not employ the *cylinder cut* in this work.

III. A^2 ASYMMETRY IN THE DECONFINEMENT PHASE

The asymmetry was introduced and studied numerically in [21] in a rather wide range of temperatures ($0.4 T_c < T < 6 T_c$). The computations were made on the lattices $16^3 \times 4$, $24^3 \times 6$, and $32^3 \times 8$. A nontrivial temperature dependence was obtained. In particular, it was found that the asymmetry is positive at $T < 2.21(5)T_c$ and negative at $T > 2.21(5)T_c$. This observation was considered as an indication that at high temperatures magnetic fluctuations begin to dominate. Comparing data for three lattice spacings the authors concluded that finite lattice spacing effects are small even for $N_t = 4$. This allows us to assume that our results obtained on lattices with $N_t = 8$ are also free of substantial finite lattice spacing effects.

Let us note that in [21] (as well as in this work) the temperature was changed by variation of the lattice spacing for fixed N_t . In Ref. [21] the finite volume effects were not checked although the spatial lattice size was decreasing with increasing temperature and

³ We assume that $D_L(p)$ and $D_T(p)$ are renormalized with the same factor.

at the highest temperature $T = 6 T_c$ it was as small as $L \equiv aN_s = 0.44$ fm with the corresponding minimal momentum $p_{min} \simeq 2.8$ GeV. In this work we carefully study the finite volume effects using lattices up to $L = 3$ fm (the detailed information on lattices used in this work is given in Table VII). Furthermore, we use Z_2 flips which help to reduce finite volume effects as was found in Ref. [48]. Here we again show that the effect of flip sectors is very substantial on small volumes. We then demonstrate that taking care about the finite volume effects dramatically changes some of the conclusions made in [21].

First, we want to reproduce the results obtained in [21] at high temperatures ($2 < T/T_c < 6$).

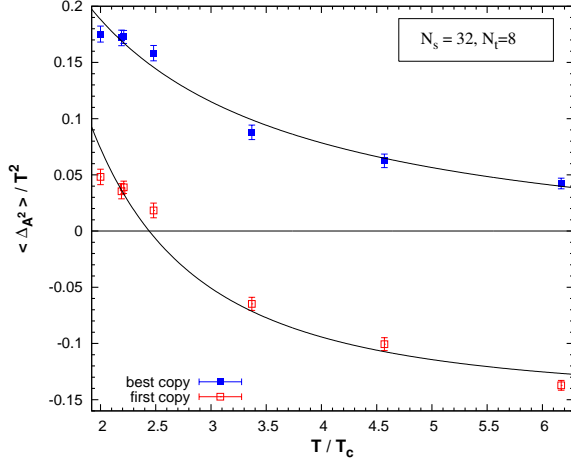


FIG. 1: Asymmetry on lattices $32^3 \times 8$ as function of temperature. Lower data set shows our results for first copy and should be compared with that obtained in [21]. Upper data set was obtained with the FSA algorithm (best copy). The curves show results of the fits to eq. (21) (for first copy) and to eq. (24) (for best copy).

In Fig.1 we show our results for \mathcal{A} obtained on lattices $32^3 \times 8$ used in [21]. Lower data set shows our results for the first copy (fc). These results are to be compared with those obtained in [21]. Upper data set corresponds to the best copy (bc). One can see that two data sets differ dramatically and this difference grows with temperature.

To make explicit comparison with [21], we fit data points corresponding to fc copy to the function

$$\mathcal{A} = b_0 + \frac{b_2}{\xi^2}, \quad (21)$$

used in [21]; here and below $\xi = T/T_c$. The parameters obtained in our fit,

$$b_0 = -0.15(1), \quad b_2 = [0.946(37)]^2, \quad (22)$$

agree well with those found in [21]:

$$b_0 = -0.164(4), \quad b_2 = [0.894(14)]^2. \quad (23)$$

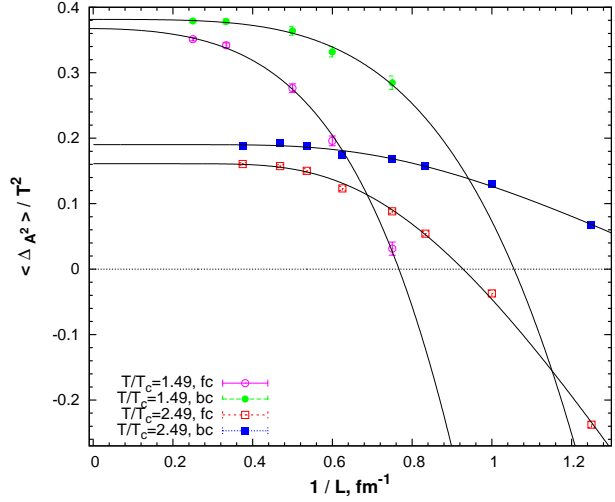


FIG. 2: Lattice size dependence of the asymmetry at $T/T_c = 1.49$ and 2.49 . Empty circles show fc results, full circles - bc results. Curves show results of the fit to eq. (27).

Our value $\xi = 2.44(13)$ at which $\mathcal{A}_{fc} = 0$ is only a little higher than the respective value $\xi = 2.21(5)$ from [21]. We conclude that our values of \mathcal{A}_{fc} come close to the values of the asymmetry obtained in [21].

Now we turn to the upper data set. It differs significantly from both the fc data set and the results of [21]. The main qualitative difference is that \mathcal{A}_{bc} does not cross zero within the range of temperatures under study. Since the difference between the two procedures employed to obtain these two data sets consists in the use of flips, we attribute the observed difference to the flip effects. As was shown in [48] the use of flips substantially reduces finite volume effects, thus we expect that the observed difference increases with a decrease of the lattice size.

In the case of bc data set the best fit is provided by the fit function

$$\mathcal{A}_{bc} \simeq b_0 + \frac{b_1}{\xi}, \quad (24)$$

with parameters

$$b_0 = -0.03(1), \quad b_1 = 0.44(3), \quad (25)$$

and $\frac{\chi^2}{N_{dof}} = 2.22$. Even if \mathcal{A}_{bc} at $N_s = 32$ becomes negative, this occurs at temperatures much greater than the upper limit of the range under our consideration.

Now we proceed to the study of the finite-volume dependence of the asymmetry and infinite volume extrapolation. In Fig.2 we show lattice-size dependence of the asymmetry at $T/T_c = 1.49$ and $T/T_c = 2.49$.

Empty symbols show the fc results, filled symbols - the bc results. As is seen in Fig.2, the volume dependence of \mathcal{A}_{fc} is very significant and at $L \simeq 1.3$ fm for $T/T_c = 1.49$ ($L \simeq 1.1$ fm for $T/T_c = 2.49$) it even changes sign. As expected the finite-size effects for \mathcal{A}_{bc} are much smaller and this is due to flips. Still the data indicate that to reduce finite-size effects below 3% one needs the minimal lattice size about 2.5 fm for both $T/T_c = 1.49$ and $T/T_c = 2.49$.

ξ	Gauge fixing algorithm	\mathcal{A}_∞^{pol}	$\sqrt{c_2}$, fm	$\sqrt[4]{c_4}$, fm	$\frac{\chi^2}{N_{dof}}$
1.49	bc	0.3828(49)	$0.1^{+0.3}_{-0.1}$	0.70(8)	0.76
1.49	fc	0.3674(64)	0.428(90)	0.92(4)	1.61
2.49	bc	0.1965(37)	0.179(40)	0.43(3)	1.99
2.49	fc	0.1834(48)	0.336(27)	0.56(2)	3.41

TABLE I: Results of fitting of the asymmetry to polynomial fit eq. (26).

To compute the asymmetry in the infinite volume limit \mathcal{A}_∞ we begin with the polynomial fit of the type

$$\mathcal{A}(L) = \mathcal{A}_\infty^{pol} - \frac{c_2}{L^2} - \frac{c_4}{L^4}, \quad (26)$$

the results are shown in Table I.

To estimate systematic errors due to choice of the fitting function, we also fitted the data to the fit function

$$\mathcal{A}(L) \simeq \mathcal{A}_\infty^{exp} - c \exp\left(-L/L_0\right) \quad (27)$$

which provides even better quality. The results of this fit are presented in Table II. One can see that the values of \mathcal{A}_∞^{pol} and \mathcal{A}_∞^{exp} agree within statistical error bars. This implies that the systematic error is of the same order as the statistical one.

ξ	Gauge fixing algorithm	\mathcal{A}_∞^{exp}	c	L_0 (fm)	$\frac{\chi^2}{N_{dof}}$
1.49	bc	0.380(2)	1.7(1.0)	0.41(5)	0.34
1.49	fc	0.352(1)	4.7(1.0)	0.47(8)	0.06
2.49	bc	0.190(2)	1.7(5)	0.31(3)	1.71
2.49	fc	0.161(2)	5.6(5)	0.31(1)	2.60

TABLE II: Results of fitting of the asymmetry to the exponential fit eq. (27).

We have also checked finite size effects for the dimension 2 electric and magnetic condensates separately. We found that the electric condensate is constant within error bars, whereas the magnetic one decreases with increasing volume. Thus the finite size

effects in the asymmetry are due to volume dependence of the magnetic condensate.

Next we consider the temperature dependence of the condensate. The results for the asymmetry in the case of fixed lattice size $L = 2$ fm and varying temperature are shown in Fig.3. We found that a good fit is provided by the function (21). The respective fit parameters are shown in Table III. It should be noted that this fit function works at $T > 1.6T_c$; at smaller temperatures terms of the order T_c^4/T^4 etc are necessary.

In Fig.3 we also show the results for the 'worst' copy which was first introduced in [49]. For a given configuration the worst copy is defined as a gauge copy with the lowest value of the gauge fixing functional. The worst copy results are to demonstrate that the Gribov copy effects within first Gribov horizon are substantially stronger than the difference between our first copy and best copy.

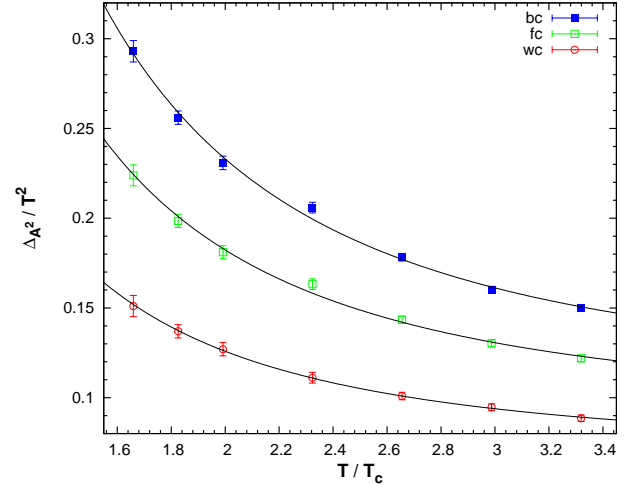


FIG. 3: Asymmetry as function of the temperature for the fixed lattice size $L = 2$ fm. The curves show the fit function (21) at the respective values of the parameters.

Using the fit function (21), we find that the asymmetry is positive at all temperatures. This is in agreement with the perturbative result (19).

The renormalized asymmetry $\mathcal{A}^{MOM} = Z_{MOM}\mathcal{A}$ where Z_{MOM} is determined in (16) can also be fitted by the function (21) with result

$$\mathcal{A}_{bc}^{MOM} = 0.0602(18) + \frac{0.268(11)}{\xi^2}, \quad \frac{\chi^2}{N_{dof}} = 0.91. \quad (28)$$

The fit was performed over the same range of temperatures.

However, the fit function (21) disagrees with the perturbative result (19) in the limit of infinite temperature where perturbation symmetry is believed to be valid. For this reason, we also fit the data to the

Gauge fixing algorithm	b_0	b_2	$\frac{\chi^2}{N_{dof}}$ $\xi > 1.65$
bc	0.1036(27)	0.517(16)	1.40
fc	0.0893(22)	0.372(13)	0.92
wc	0.0682(5)	0.231(3)	0.05

TABLE III: b_0 and b_2 are the parameters of the fit (21) performed over the range $1.65 < \xi < 3.32$ for asymmetry computed at fixed lattice size $L = 2\text{fm}$.

function (motivated by (19))

$$\mathcal{A} \simeq \frac{zg^2(T)}{4} \left(1 - \frac{g(T)}{3\pi} \sqrt{\frac{2}{3}} \right), \quad (29)$$

where the running coupling is taken in the two-loop approximation,

$$\frac{1}{g^2(T)} = \frac{1}{4\pi^2} \left(\frac{11}{6} \ln \left(\frac{T^2}{\Lambda^2} \right) + \frac{17}{11} \ln \ln \left(\frac{T^2}{\Lambda^2} \right) \right), \quad (30)$$

z and Λ are the fit parameters.

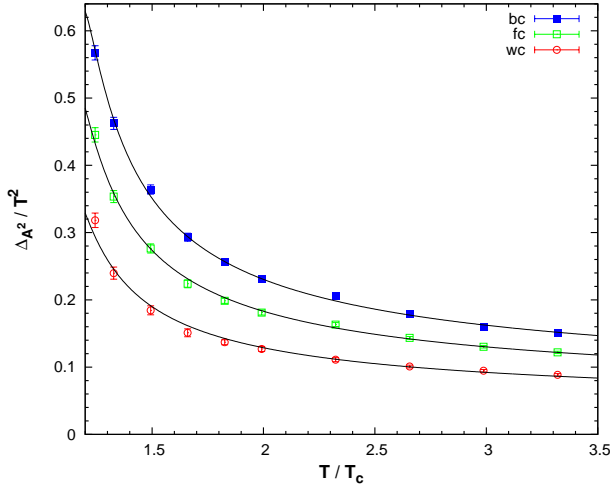


FIG. 4: Same as in Fig. 3 but \mathcal{A} is fitted to the function (29); also wider range of temperatures is shown.

The results of the fit over the range $1.24 < \xi < 3.32$ are shown in Table IV. Note that it works over wider range of temperatures than the fit (21).

Therefore, we arrive at a good agreement with perturbation theory modulo the normalization factor of the propagator. In order to make quantitative comparison with the perturbative result, we should use the same normalization condition; however, the \overline{MS}

Gauge fixing algorithm	z	Λ/T_c	$\frac{\chi^2}{N_{dof}}$ $\xi > 1.24$
bc	0.1284(14)	0.845(7)	1.50
fc	0.1045(13)	0.826(7)	1.12
wc	0.0749(17)	0.811(14)	1.93

TABLE IV: Parameters of the fit of the asymmetry to eq. (29).

scheme employed in [44] runs into difficulties beyond perturbation theory.

Thus we infer that, contrary to the conclusions of Ref. [21], the asymmetry never crosses zero in the deconfining phase. Accordingly it cannot indicate the boundary between two regions of the deconfining phase, whose existence was discussed in [27, 30, 31, 50, 51].

IV. RATIO $D_T(0)/D_L(0)$

It is natural to expect that the existence of the postconfinement region is explained by the contribution of low-momentum, i.e. nonperturbative, modes of the gauge field. This motivates us to consider in this work the ratio of the magnetic to electric propagator at zero momentum as a possible indicator of the boundary of the postconfinement region.

Similar ratio of electric and magnetic screening masses was computed in [52]. These masses were evaluated in [52] (see analogous computation in $SU(3)$ gluodynamics in [32]) in a renormalization-invariant way, by long-distance behavior of the gluon propagators:

$$\begin{aligned} \tilde{D}_L(p_\perp = 0, x_3) &\sim \exp(-m_e|x_3|), \\ \tilde{D}_T(p_\perp = 0, x_3) &\sim \exp(-m_m|x_3|), \quad |x_3| \rightarrow \infty \end{aligned} \quad (31)$$

where $\tilde{D}_L(p_\perp, x_3)$ and $\tilde{D}_T(p_\perp, x_3)$ are, respectively, the Fourier transforms of $D_L(p)$ and $D_T(p)$ in the third component of the momentum. There are different views on gauge invariance of these masses — even in the framework of perturbation theory: the authors of [52] consider them gauge-independent, whereas the authors of [43] cast some doubt on both their gauge-invariance and physical meaning.

In the leading-order perturbation theory $m_e = \sqrt{\frac{2}{3}}g(T)T$ in the $SU(2)$ case, whereas for m_m (which is of nonperturbative nature) the behavior $g^2(T)T$ is conjectured. The authors of [52] obtained the data for

$T > 2T_c$ and employed fit formula

$$\frac{m_e^2(T)}{m_m^2(T)} = \frac{C}{g^2(T)}. \quad (32)$$

Let us note that the authors of [52] did not take care of finite size effects. In their study the lattice size was decreasing with an increase of the temperature similar to Ref. [21]. Over the temperature range explored in our study, their lattice size decreased from 2 fm down to 0.8 fm.

In the present work we consider the ratio $r(T) = \frac{D_T(0)}{D_L(0)}$ instead of $\frac{m_e^2}{m_m^2}$. Our arguments are as follows. It was shown in [53] that the low momentum behavior of $D_L(p)$ is compatible with pole behavior and renormalized $D_L(0)$ can be considered as inverse electric mass squared. However, the low momentum behavior of $D_T(p)$ is definitely different from the pole behavior. It has a maximum at nonzero momentum $p_0 \sim 0.4 \div 0.5$ GeV, see, e.g. Fig. 8 in [53]. Still $D_T(0)$ characterizes the strength of $D_T(p)$ at low momentum⁴ We assume that the temperature T_p satisfying relation

$$r(T_p) = 1; \quad (33)$$

determines the boundary of the postconfinement region. This is not a phase transition thus the boundary is not characterized by definite value of the temperature but rather by a range of temperature values.

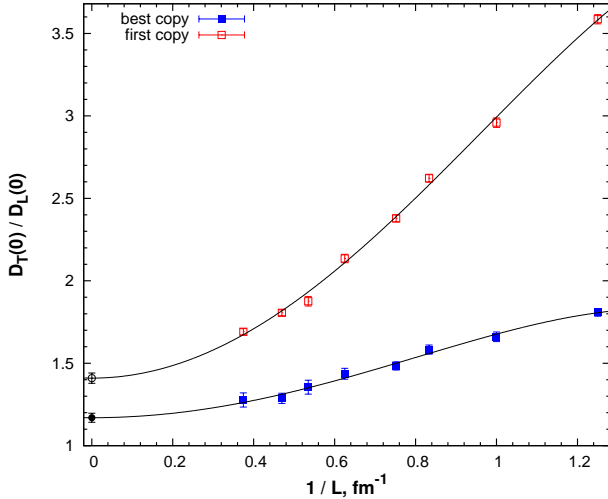


FIG. 5: Lattice size dependence of the ratio $r(T)$ for first copies (empty symbols) and best copies (filled symbols) at $T/T_c = 2.49$.

We start from the study of the finite size effects for $r(T)$. In Fig. 5 we show the ratio as the function of the inverse lattice size $1/L$ for $T/T_c = 2.49$ for first copies (empty symbols) and best copies (filled symbols). The difference between two data sets is huge on small volumes and decreases with increasing volume. As in the case of the asymmetry (see Fig. 2) this difference is due to application of the flip procedure. For best copies the finite size effects are much smaller than for the first copies but they are still sizable up to lattice size L about 2 fm. For $L = 3$ fm lattice finite size correction is small and comparable to statistical error. We fit the lattice size dependence of $r(T)$ to the polynomial fit as in the case of asymmetry

$$r(T, L) = r(T, \infty) + \frac{r_2(T)}{L^2} + \frac{r_4(T)}{L^4}. \quad (34)$$

The result is as follows:

$$\begin{aligned} bc: \quad r(2.49 T_c, \infty) &= 1.170(27), \quad \frac{\chi^2}{N_{dof}} = 0.57; \\ fc: \quad r(2.49 T_c, \infty) &= 1.410(31), \quad \frac{\chi^2}{N_{dof}} = 2.12. \end{aligned} \quad (35)$$

Results of the fits are presented in Fig. 5. The fits predict that the difference between $r(T)$ values obtained via two gauge fixing procedures survives in the infinite volume limit.

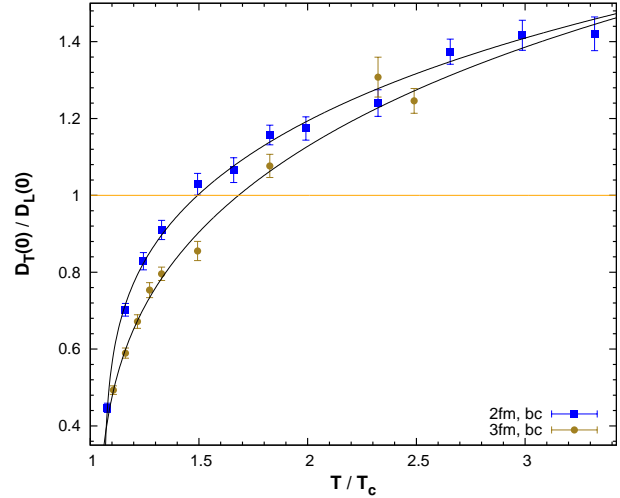


FIG. 6: Ratio $r(T)$ for best copies on lattices with fixed sizes $L = 2$ fm and $L = 3$ fm versus temperature. Fits to eq. 36 are also shown.

The best copy ratio $r(T)$ for two fixed lattice sizes $L = 2$ fm and $L = 3$ fm versus temperature is plotted in Fig. 6. Note that the point on $L = 3$ fm lattice at the largest temperature $T = 2.49T_c$ was obtained by the extrapolation shown in Fig. 5. The data presented in this figure indicate that the finite size effect is definitely nonzero up to $T/T_c = 1.8$ and might disappear at higher temperatures.

⁴ Note that Linde [54] related the magnetic mass to transverse gluon propagator at zero momentum.

We fit the T dependence of $r(T)$ to the function

$$r(T) \simeq r_0 + \frac{r_1}{g^2(T)}, \quad (36)$$

inspired by eq. (32). Here $r_0, r_1, \Lambda/T_c$ are the fit parameters. This fit formula works surprisingly well at $T > 1.08T_c$ as can be seen from Fig.6 and Table V.

Lattice size	r_0	r_1	Λ/T_c	T_p/T_c	$\frac{\chi^2}{N_{dof}}$
2 fm	0.94(1)	3.78(12)	1.060(3)	1.494(30)	0.64
3 fm	0.79(3)	4.59(37)	1.02(2)	1.68(12)	1.42

TABLE V: Parameters of the fit of the ratio $r(T)$ for best copies on lattices with $L = 2$ fm and $L = 3$ fm to fit function (36).

It should be noted that the fit formula (36) works well for all $T > \Lambda$ - even in the case when the coupling $g^2(T)$ (30) becomes negative at T/T_c below 1.4. However, this motivates us to employ yet another fit function

$$r(T) \simeq R_0 + R_1 \ln \left(\frac{T}{T_c} - 1 \right) \quad (37)$$

The results of this fit are shown in Fig.7 and in Table VI. It is clearly seen that this simple logarithmic fit function works also well. The slope is independent of the volume, whereas the intercept slowly decreases with an increase of lattice size. We have every reason to consider $L = 3$ fm as a good approximation to the infinite-volume limit (cf. Fig. 5). The values of T_p/T_c obtained with two fits agree within error bars.

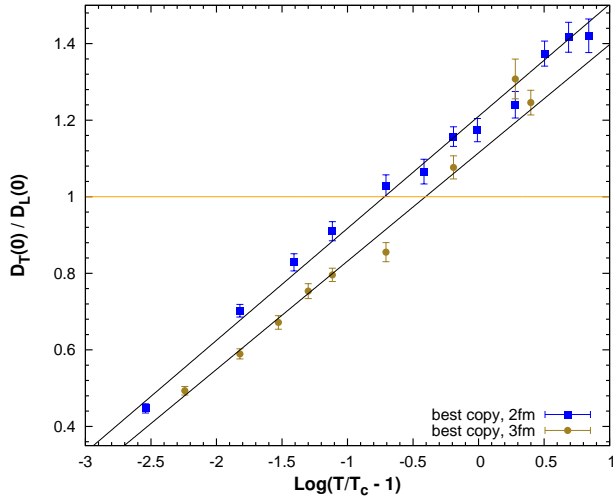


FIG. 7: Ratio $r(T)$ for best copies on lattices with fixed sizes $L = 2$ fm and $L = 3$ fm versus $\log(T/T_c - 1)$ with fits to eq. 37.

The fit function (37) can be rearranged to the form

$$r(T) \simeq R_1 \ln \left(\frac{T - T_c}{Q} \right), \quad (38)$$

where Q sets the scale over the postconfinement domain. We find that $Q \approx 230$ MeV, which comes close to the quantity $m = 201(8)$ MeV [21] that sets the temperature scale for the asymmetry at low temperatures in the confinement phase.

Lattice size	R_0	R_1	T_p/T_c	$\frac{\chi^2}{N_{dof}}$
2 fm	1.21(1)	0.293(6)	1.488(13)	1.35
3 fm	1.115(15)	0.283(9)	1.667(27)	1.92

TABLE VI: Parameters of the fit of the ratio $r(T)$ for best copies on lattices with $L = 2$ fm and $L = 3$ fm to fit function (37).

The difference between the parameters in Tables V and VI gives an estimate of the systematic error in determination of T_p defined by the formula (33).

The fit functions (36) and (37) imply that the ratio $D_T(0)/D_L(0)$ goes to infinity in the infinite temperature limit. Results at higher temperatures are needed to confirm this prediction.

V. CONCLUSIONS

We presented results of the study of the asymmetry \mathcal{A} and the ratio $D_T(0)/D_L(0)$ in lattice $SU(2)$ gluodynamics on lattices with varying spatial size N_s in the range of temperatures above T_c up to $3.3T_c$. Our findings can be summarized as follows:

- In contrast to conclusions made in [21] the asymmetry is positive at all temperatures under consideration and its high-temperature behavior agrees with perturbation theory. The data can be fitted to function motivated by the perturbation theory down to temperatures as low as $1.25T_c$. The asymmetry cannot be used as indicator of the postconfinement domain boundary.
- A good indicator of the boundary of the postconfinement domain is provided by $D_T(0)/D_L(0)$ rather than by the asymmetry \mathcal{A} . The transition temperature T_p defined by the condition $D_T(0)/D_L(0) = 1$ slightly increases with increasing volume. At $L = 3$ fm, which is close to the infinite-volume limit, $T_p = 1.68(12)T_c$.
- In the range of temperatures under study in this work the effect of flip sectors is substantial at

$L \simeq 2$ fm and crucial at $L < 1$ fm. In the latter case, it dramatically changes the behavior of both the asymmetry and ratio $D_T(0)/D_L(0)$.

- Finite-volume effects are significant on lattices with $L < 2$ fm within our range of temperatures and decrease with increasing temperature.
- The temperature dependence of the ratio $D_T(0)/D_L(0)$ can well be fitted by both the perturbatively motivated function (36) and the linear function of $\ln(T - T_c)$ (38) over the range

$$1.08T_c < T < 3.32T_c.$$

Acknowledgments

Computer simulations were performed on the IHEP (Protvino) Central Linux Cluster, ITEP (Moscow) Linux Cluster, MSU 'Lomonosov' supercomputer. The work was supported by the Russian Foundation for Basic Research, grant no.16-02-01146 A.

-
- [1] F. V. Gubarev, L. Stodolsky, and V. I. Zakharov, Phys. Rev. Lett. **86**, 2220 (2001), hep-ph/0010057.
 - [2] M. J. Lavelle and M. Schaden, Phys. Lett. **B208**, 297 (1988).
 - [3] H. Verschelde, K. Knecht, K. Van Acoleyen, and M. Vanderkelen, Phys. Lett. **B516**, 307 (2001), hep-th/0105018.
 - [4] D. Dudal, H. Verschelde, V. E. R. Lemes, M. S. Sarandy, R. F. Sobreiro, S. P. Sorella, and J. A. Gracey, Phys. Lett. **B574**, 325 (2003), hep-th/0308181.
 - [5] A. A. Slavnov, Theor. Math. Phys. **143**, 489 (2005), [Teor. Mat. Fiz.143,3(2005)], hep-th/0407194.
 - [6] D. V. Bykov and A. A. Slavnov, Theor. Math. Phys. **145**, 1495 (2005), [Teor. Mat. Fiz.145,147(2005)], hep-th/0505089.
 - [7] R. E. Browne and J. A. Gracey, JHEP **11**, 029 (2003), hep-th/0306200.
 - [8] P. Boucaud, J. P. Leroy, A. L. Yaouanc, J. Micheli, O. Pene, and J. Rodriguez-Quintero, Few Body Syst. **53**, 387 (2012), 1109.1936.
 - [9] K. Petrov, B. Blossier, P. Boucaud, O. Pene, M. Brinet, F. de Soto, V. Morenas, and J. Rodriguez-Quintero, PoS **ConfinementX**, 043 (2012), 1304.3296.
 - [10] P. Boucaud, M. Brinet, F. De Soto, V. Morenas, O. Pene, K. Petrov, and J. Rodriguez-Quintero, JHEP **04**, 086 (2014), 1310.4087.
 - [11] P. Boucaud, A. Le Yaouanc, J. P. Leroy, J. Micheli, O. Pene, and J. Rodriguez-Quintero, Phys. Lett. **B493**, 315 (2000), hep-ph/0008043.
 - [12] P. Boucaud, F. De Soto, J. P. Leroy, A. Le Yaouanc, J. Micheli, O. Pene, and J. Rodriguez-Quintero, Phys. Rev. **D79**, 014508 (2009), 0811.2059.
 - [13] O. Pene et al., PoS **FACESQCD**, 010 (2010), 1102.1535.
 - [14] B. Blossier, P. Boucaud, M. Brinet, F. De Soto, V. Morenas, O. Pene, K. Petrov, and J. Rodriguez-Quintero (ETM), Phys. Rev. **D89**, 014507 (2014), 1310.3763.
 - [15] D. Dudal, J. A. Gracey, S. P. Sorella, N. Vandersickel, and H. Verschelde, Phys. Rev. **D78**, 065047 (2008), 0806.4348.
 - [16] D. Dudal, O. Oliveira, and N. Vandersickel, Phys. Rev. **D81**, 074505 (2010), 1002.2374.
 - [17] A. Cucchieri, D. Dudal, T. Mendes, and N. Vandersickel, Phys.Rev. **D85**, 094513 (2012), 1111.2327.
 - [18] K.-I. Kondo, Phys. Lett. **B514**, 335 (2001), hep-th/0105299.
 - [19] D. Dudal, H. Verschelde, and S. P. Sorella, Phys. Lett. **B555**, 126 (2003), hep-th/0212182.
 - [20] E. Ruiz Arriola, P. O. Bowman, and W. Broniowski, Phys. Rev. **D70**, 097505 (2004), hep-ph/0408309.
 - [21] M. N. Chernodub and E. M. Ilgenfritz, Phys. Rev. **D78**, 034036 (2008), 0805.3714.
 - [22] P. Chakraborty and M. G. Mustafa, Phys. Lett. **B711**, 390 (2012), 1203.2068.
 - [23] F. Karsch, Lect. Notes Phys. **583**, 209 (2002), hep-lat/0106019.
 - [24] O. Kaczmarek, F. Karsch, P. Petreczky, and F. Zantow, Phys. Lett. **B543**, 41 (2002), hep-lat/0207002.
 - [25] A. Dumitru, Y. Hatta, J. Lenaghan, K. Orginos, and R. D. Pisarski, Phys. Rev. **D70**, 034511 (2004), hep-th/0311223.
 - [26] M. Asakawa and T. Hatsuda, Phys. Rev. Lett. **92**, 012001 (2004), hep-lat/0308034.
 - [27] A. Dumitru, Y. Guo, Y. Hidaka, C. P. K. Altes, and R. D. Pisarski, Phys. Rev. **D83**, 034022 (2011), 1011.3820.
 - [28] Y. Hidaka, S. Lin, R. D. Pisarski, and D. Satow, JHEP **10**, 005 (2015), 1504.01770.
 - [29] Y. Hidaka and R. D. Pisarski, Phys. Rev. **D78**, 071501 (2008), 0803.0453.
 - [30] J. Liao and E. Shuryak, Phys. Rev. **C75**, 054907 (2007), hep-ph/0611131.
 - [31] M. N. Chernodub and V. I. Zakharov, Phys. Rev. Lett. **98**, 082002 (2007), hep-ph/0611228.
 - [32] A. Nakamura, T. Saito, and S. Sakai, Phys. Rev. **D69**, 014506 (2004), hep-lat/0311024.
 - [33] V. K. Mitrjushkin, A. M. Zadorozhnyi, and G. M. Zinovev, Phys. Lett. **B215**, 371 (1988).
 - [34] T. Appelquist and R. D. Pisarski, Phys. Rev. **D23**, 2305 (1981).
 - [35] P. H. Ginsparg, Nucl. Phys. **B170**, 388 (1980).
 - [36] E. Braaten and A. Nieto, Phys. Rev. **D53**, 3421 (1996), hep-ph/9510408.
 - [37] K. Kajantie, M. Laine, K. Rummukainen, and Y. Schroder, Phys. Rev. **D67**, 105008 (2003), hep-ph/0211321.
 - [38] M. Laine and Y. Schroder, JHEP **03**, 067 (2005), hep-ph/0503061.
 - [39] P. N. Meisinger, T. R. Miller, and M. C. Ogilvie, Phys. Rev. **D65**, 034009 (2002), hep-ph/0108009.
 - [40] R. D. Pisarski, Phys. Rev. **D74**, 121703 (2006), hep-

- ph/0608242.
- [41] P. de Forcrand, A. Kurkela, and A. Vuorinen, Phys. Rev. **D77**, 125014 (2008), 0801.1566.
 - [42] J. E. Mandula and M. Ogilvie, Phys. Lett. **B185**, 127 (1987).
 - [43] J. Kapusta and C. Gale, *Finite-Temperature Field Theory: Principles and Applications* (Cambridge University Press, Cambridge CB2 2RU UK, 2006).
 - [44] D. Vercauteren and H. Verschelde, Phys. Rev. **D82**, 085026 (2010), 1007.2789.
 - [45] I. L. Bogolubsky, G. Burgio, V. K. Mitrjushkin, and M. Müller-Preussker, Phys. Rev. **D74**, 034503 (2006), hep-lat/0511056.
 - [46] V. G. Bornyakov, V. K. Mitrjushkin, and M. Muller-Preussker (2009), 0912.4475.
 - [47] Y. Nakagawa, A. Voigt, E. M. Ilgenfritz, M. Muller-Preussker, A. Nakamura, T. Saito, A. Sternbeck, and H. Toki, Phys. Rev. **D79**, 114504 (2009), 0902.4321.
 - [48] I. L. Bogolubsky, V. G. Bornyakov, G. Burgio, E. M. Ilgenfritz, M. Muller-Preussker, and V. K. Mitrjushkin, Phys. Rev. **D77**, 014504 (2008), [Erratum: Phys. Rev.D77,039902(2008)], 0707.3611.
 - [49] V. Bornyakov, V. Mitrjushkin, and R. Rogalyov, Phys.Rev. **D89**, 054504 (2014), 1304.8130.
 - [50] J. Liao and E. Shuryak, Phys. Rev. Lett. **101**, 162302 (2008), 0804.0255.
 - [51] M. N. Chernodub and V. I. Zakharov, Phys. Atom. Nucl. **72**, 2136 (2009), 0806.2874.
 - [52] U. M. Heller, F. Karsch, and J. Rank, Phys. Rev. **D57**, 1438 (1998), hep-lat/9710033.
 - [53] V. Bornyakov and V. Mitrjushkin, Phys.Rev. **D84**, 094503 (2011), 1011.4790.
 - [54] A. D. Linde, Phys. Lett. **B96**, 289 (1980).

Appendix: Table of statistics

β	N_s	L (fm)	a^{-1} (GeV)	T (MeV)	T/T_c	n_{copy}	n_{meas}
2.5574	28	2.00	2.7622	345.3	1.162	1	1780
2.5792	30	2.00	2.9595	369.4	1.245	1	1246
2.5996	32	2.00	3.1568	394.6	1.328	1	1068
2.6370	36	2.00	3.5514	443.9	1.494	1	1157
2.6706	40	2.00	3.9460	493.3	1.660	1	979
2.7011	44	2.00	4.3406	542.6	1.826	1	1744
2.7290	48	2.00	4.7352	591.9	1.992	1	1246
2.7788	56	2.00	5.5244	690.6	2.324	1	1068
2.8221	64	2.00	6.3136	789.2	2.656	2	1467
2.8604	72	2.00	7.1028	887.9	2.987	2	1132
2.8949	80	2.00	7.8920	986.5	3.319	3	927
2.8011	24	0.80	5.919	739.9	2.490	1	3560
2.8011	36	1.20	5.919	739.9	2.490	1	2816
2.8011	40	1.33	5.919	739.9	2.490	1	2848
2.8011	48	1.60	5.919	739.9	2.490	1	801
2.8011	56	1.87	5.919	739.9	2.490	1	880
2.8011	64	2.13	5.919	739.9	2.490	2	693
2.8011	80	2.67	5.919	739.9	2.490	3	740
2.7310	32	1.33	4.764	595.5	2.00	1	1068
2.7600	32	1.21	5.213	651.6	2.19	1	1068
2.7630	32	1.20	5.261	657.6	2.21	1	1691
2.8000	32	1.07	5.899	773.4	2.48	1	1068
2.9000	32	0.79	8.016	1002	3.37	1	1068
3.0000	32	0.58	10.86	1357	4.57	1	1068
3.1000	32	0.43	14.68	1835	6.17	1	1780
2.5421	40	3.00	2.6307	328.8	1.106	1	1758
2.5574	42	3.00	2.7622	345.3	1.162	1	1780
2.5721	44	3.00	2.8937	361.7	1.106	1	1273
2.5861	46	3.00	3.0253	378.2	1.106	1	1412
2.5996	48	3.00	3.1568	394.6	1.328	1	1780
2.7011	66	3.00	4.3406	542.6	1.826	2	1011
2.6370	24	1.33	3.5514	443.9	1.494	1	1709
2.6370	30	1.67	3.5514	443.9	1.494	1	1660
2.6370	36	2.00	3.5514	443.9	1.494	1	1157
2.6370	48	1.67	3.5514	443.9	1.494	1	1780
2.6370	54	3.00	3.5514	443.9	1.494	1	1068
2.6370	72	4.00	3.5514	443.9	1.494	2	974

TABLE VII: Values of β , lattice sizes, temperatures, number of measurements and number of gauge copies used throughout this paper. To fix the scale we take $\sqrt{\sigma} = 440$ MeV.